



저작자표시 2.0 대한민국

이용자는 아래의 조건을 따르는 경우에 한하여 자유롭게

- 이 저작물을 복제, 배포, 전송, 전시, 공연 및 방송할 수 있습니다.
- 이차적 저작물을 작성할 수 있습니다.
- 이 저작물을 영리 목적으로 이용할 수 있습니다.

다음과 같은 조건을 따라야 합니다:



저작자표시. 귀하는 원저작자를 표시하여야 합니다.

- 귀하는, 이 저작물의 재이용이나 배포의 경우, 이 저작물에 적용된 이용허락조건을 명확하게 나타내어야 합니다.
- 저작권자로부터 별도의 허가를 받으면 이러한 조건들은 적용되지 않습니다.

저작권법에 따른 이용자의 권리는 위의 내용에 의하여 영향을 받지 않습니다.

이것은 [이용허락규약\(Legal Code\)](#)을 이해하기 쉽게 요약한 것입니다.

[Disclaimer](#) 

Master's Thesis of Science in Agriculture

**Morphological and Molecular Characterization of
Mutants with Distorted Trichomes in Tomato**

토마토에서 뒤틀린 모상체를 가진 돌연변이의
형태학 그리고 분자적 특성 규명

August 2019

Jae-In Chun

**Department of International Agricultural Technology
Graduate School of International Agricultural Technology
Seoul National University**

Abstract

Morphological and Molecular Characterization of Mutants with Distorted Trichomes in Tomato

Jae-In Chun

Major of International Agricultural Technology
Department of International Agricultural Technology
Graduate School of International Agricultural Technology
Seoul National University

Trichomes are hair-like structures on the aerial surface of many plant species. Trichomes are well characterized for their function as physical and chemical defense against biotic and abiotic stresses. Despite the important roles of trichomes in plant defense, most of the genes for multicellular trichome formation including tomato remain unknown. To identify genes related to trichome development in tomato, we screened Micro-Tom mutant population generated by Ethylmethane sulfonate (EMS) mutagenesis and obtained four mutants with distinct trichome phenotypes compared with wild-type (WT) Micro-Tom plants. All mutants that we obtained have a similar trichome morphology with distorted and curled trichomes like previously known tomato mutants *hairless* (*hl*) and *inquieta* (*ini*). So we designated the new mutants as *hl2*, *hl3*, *hl4*, and *hl5*. Here, we describe the characterization of the new mutants in detail. Previously, we demonstrated that *Hl* and *Ini* genes are involved in the polymerization of actin cytoskeleton. Given similar trichome morphology among the new mutants, *hl*, and *ini*, we hypothesized that genes corresponding to the new four

mutants are also related to actin polymerization. We performed reverse transcription (RT)-PCR from the new four mutant leaves using 16 specific primer set for actin-related protein (*ARP*)2/3 and *WAVE* complex genes which are involved in actin polymerization. All genes were amplified with expected size in the four mutants except for *ARPC1* gene which showed different fragment size between WT and *hl5* plants. cDNA and genomic DNA sequencing of *ARPC1* gene revealed that a single base substitution of G to A at the 5'-donor site of the intron 9 in *hl5* mutant caused missplicing and generated premature stop codon. We demonstrated that expression of a WT *ARPC1* cDNA in the *hl5* mutant background recovered normal trichome development. These results establish a role for *ARPC1* in the development of tomato trichomes and also implicate the actin-cytoskeleton network in trichome morphogenesis.

.....
Keywords : Actin, ARP2/3-WAVE complex, ARPC1, *Hairless*, Tomato (*Solanum lycopersicum*), Trichome

Student Number : 2017-23619

Contents

Abstract	i
Contents	iii
List of Figures	iv
List of Tables	v
List of Abbreviations	vi
Introduction	1
Materials and Methods	4
1. Plant materials and growth conditions	4
2. Analysis of trichome morphology	4
3. RT-PCR and genomic DNA PCR	5
4. Amino acid alignment and phylogenetic analysis	6
5. Vector construct	6
6. Tomato transformation	7
7. Transgenic plants for complementary test	8
Results	9
1. Screening of Micro-Tom mutants related to trichome development	9
2. RT-PCR analysis of tomato homologs of the ARP2/3-WAVE complex in <i>hl2</i> , <i>hl3</i> , <i>hl4</i> , and <i>hl5</i> mutants	9
3. <i>hl5</i> affects trichome development	10
4. <i>HL5</i> encodes the tomato homolog of ARPC1	11
5. Comparison of ARPC1 homologs between tomato and other species	12
6. Genetic complementation of the <i>hl5</i> mutant restores normal trichome development	12
Discussion	28
References	32
Abstract in Korean	40

List of Figures

Figure 1. Light micrographs of trichomes in wild-type (WT) and distorted mutants	13
Figure 2. RT-PCR analysis on the 14 tomato homologs of the ARP2/3-WAVE complex genes	14
Figure 3. Light micrographs of trichomes on the leaf, stem, hypocotyl, and sepal of wild-type (WT), <i>hl5</i> , <i>hl</i> , and <i>ini</i> plants	15
Figure 4. SEM micrographs of trichomes on the leaf, stem, hypocotyl, and sepal of wild-type (WT), <i>hl5</i> , <i>hl</i> , and <i>ini</i> plants	16
Figure 5. The <i>Hl5</i> gene encodes ARPC1	17
Figure 6. Comparison of <i>ARPC1</i> cDNA sequence between wild-type (WT) and <i>hl5</i> mutant	18
Figure 7. Alignment of ARPC1 amino acids sequence from wild-type (WT) and <i>hl5</i> plants	20
Figure 8. Comparison of <i>ARPC1</i> genomic DNA sequence between wild-type (WT) and <i>hl5</i> plants	21
Figure 9. Similarity of ARPC1 between tomato and other species	22
Figure 10. <i>ARPC1</i> complements the trichome morphology defect of the <i>hl5</i> mutant	25

List of Tables

Table 1. Arabidopsis genes encoding subunits of the ARP2/3-WAVE complexes and their homolog genes in tomato	26
Table 2. List of primer sequences used in this study	27

LIST OF ABBREVIATIONS

AS	Alternative Splicing
ARP2/3	Actin-related protein
bHLH	basic helix-loop-helix
<i>CaMV35s</i>	<i>Cauliflower mosaic virus 35S promoter</i>
cDNA	Complementary deoxyribonucleic acid
<i>dis</i>	<i>distorted</i>
EMS	Ethylmethane sulfonate
gDNA	Genomic deoxyribonucleic acid
GIS	GLABROUS INFLORESCENCE STEMS
<i>Hl</i>	<i>Hairless</i>
<i>Ini</i>	<i>Inquieta</i>
mRNA	Messenger ribonucleic acid
NOS	Nopaline synthase
PCR	Polymerase chain reaction
RNA	Ribonucleic acid
RT-PCR	Reverse transcription polymerase chain reaction
SEM	Scanning Electron Microscopy

T-DNA	Transfer deoxyribonucleic acid
WDR	WD40 repeat
WT	Wild-type
ZFPs	C2H2 zinc finger proteins

Introduction

Trichomes are fine outgrowths derived from epidermal cells on the leaf, hypocotyl, stem, and floral organs of plant species. They perform diverse biological functions such as protection against biotic stresses, including insect and pathogen attack (Kennedy 2003; Shepherd et al. 2005) and adaptation to abiotic stresses such as water loss and UV-B radiation (Ehleringer and Mooney 1978; Karabourniotis et al. 1992). Trichomes are normally classified as being either non-glandular or glandular and either unicellular or multicellular and may vary in size, shape, number of cells, morphology, and chemical composition (Goffreda et al. 1989; Kang et al. 2010a, b; Schimiller et al. 2009; Nonamua et al. 2008; Tian et al. 2012). As trichomes are easily accessible to a combination of genetic, cell biological and molecular methods they have become an ideal model system to study various aspects of plant cell morphogenesis (Schwab et al. 2000).

As a model plant, *Arabidopsis* has been well studied for transcriptional regulatory network in the initiation and development of trichomes through genetic and molecular analysis. Trichome development is controlled by a trimeric transcriptional complex consisting of R2R3 MYB proteins, basic helix-loop-helix (bHLH) proteins, and a WD40 repeat (WDR) protein. This MYB-bHLH-WDR complex positively regulates the expression of the homeodomain transcription factor *GL2* to regulate trichome initiation (Szymanski et al. 1998; Ramsay and Glover 2005; Zhao et al. 2008). Recently, C2H2 zinc finger proteins (ZFPs) including *GLABROUS INFLORESCENCE STEMS* (*GIS*) and *ZFP5* were identified as upstream transcriptional regulators to control the expression of MYB or bHLH genes (Gan et al. 2006; Yan et al. 2014). After trichome formation is initiated, trichome cells are enlarged and develop branches by arresting cell division and switching to the endoreplication cycles, which are genetically controlled by several different genes including *SIAMESE* and *ZWICHEL* (Oppenheimer et al. 1997; Walker et al. 2000;

Grebe 2012). Finally, the actin-related protein (ARP)2/3 complex involved in nucleating actin filaments, and the WAVE complex that regulates ARP2/3 activity, are required to maintain polarized stalk and branch growth. The ‘distorted group’ mutants were identified based on the aborted branch and swollen phenotype (Szymanski, 2000) and these genes encode subunits of two different complexes that directly regulate the actin cytoskeleton; ARP2/3 complex that nucleates actin filaments and the WAVE complex that regulates the activity of ARP2/3 (Szymanski, 2005).

Cultivated tomato (*Solanum lycopersicum L.*) and its wild relatives have at least seven distinct types of trichomes that differ with respect to size, cell number, and the presence of glandular secreting cells (Luckwill 1943). Among the non-glandular trichome types (type II, III, and V), type II and type III trichomes are similar in length but differ by the presence of a multicellular and unicellular base, respectively. The shortest type V trichomes have a unicellular base. Among four different glandular trichomes (type I, IV, VI, and VII), type I trichomes have a multicellular base, a long multicellular stalk, and a small glandular tip. Type IV trichomes contain a unicellular base, a short multicellular stalk, and a small secreting glandular tip. Type VI trichomes consist of a four-celled glandular head on a short multicellular stalk, whereas type VII trichomes have a unicellular stalk and an irregularly shaped 4- to 8-celled gland (Luckwill 1943; Kang et al. 2010). The glandular trichomes have been well characterized as chemical “factories” that produce diverse specialized metabolites implicated in anti-insect defense. For instance, terpenoids, flavonoids, 2-tridecanone and other methyl ketones synthesized in type VI trichomes of cultivated tomato and its wild relatives exert toxic effects on several arthropod pests, including tobacco hornworm (*Manduca sexta*), aphids (*Macrosiphum euphorbiae* and *Myzus persicae*), and Colorado potato beetle (*Leptinotarsa decemlineata*) (Williams et al. 1980; Kennedy 2003; Kang et al. 2010b). Acyl sugars secreted from type IV trichomes of *S. pennellii* play an important role in the

resistance to numerous insects such as whiteflies (*Bemisia argentifolii* and *Trialeurodes vaporariorum*), beet armyworm (*Spodoptera exigua*), tomato fruitworms, and aphids (Goffreda et al. 1990; Rodriguez et al. 1993; Juvik et al. 1994; Kennedy 2003). Given the important roles of these compounds in plant protection, recent research has focused on understanding the underlying biochemical pathways required for their synthesis (Sallaud et al. 2009; Schilmiller et al. 2009; Bleeker et al. 2012; Schilmiller et al. 2012; Kang et al. 2014). However, our understanding of how multicellular trichomes develop is still in its infancy and only a few genes controlling trichome development have been identified. For example, the *Woolly* gene encoding a homeodomain-containing transcription factor regulates type I trichome development (Yang et al. 2011). The *Hairless (Hl)* gene encoding the *SRA1* subunit of the WAVE regulatory complex is required for proper cell enlargement and cell shape of all trichome types in tomato (Kang et al. 2016). The *Inquieta (Ini)* gene was identified that encodes the *ARPC2A* involved in nucleating the polymerization of actin filaments (Jeong et al. 2017).

The *hl5* mutant was generated by Ethylmethane sulfonate (EMS) mutagenesis from Micro-Tom (Watanabe et al. 2007). The *hl5* mutant has a phenotype of distorted and curled trichomes on all tissues. Previous studies showed that *hairless* and *iniquieta* mutants have distorted trichomes and the corresponding genes are involved in the polymerization of actin cytoskeleton (Kang et al. 2016; Jeong et al. 2017). So we predicted that the *hl5* mutant is also related to actin polymerization.

In this paper, we were able to do both analysis of trichome morphology of *hl5* mutant and also identification of *Hl5* gene. Our results show that the *ARPC1* gene, which encodes a subunit of ARP2/3 complex corresponds to *hl5* mutant. Molecular analysis revealed a point mutation occurred in *ARPC1* gene of *hl5* mutant plants. This mutation in exon 9 led to premature termination codons by skipping the entire forward exon. These findings provide compelling evidence that altered trichome development in the *hl5* mutant is caused by a defect in *ARPC1*.

Materials and methods

1. Plant materials and growth conditions

Tomato (*Solanum lycopersicum*) cv Micro-Tom (accession number LA3911) was used as the wild type (WT) for all experiments. Seeds for WT and EMS mutagenized mutant *hl2*, *hl3*, *hl4*, and *hl5* (accession number TOMJPW4375) were obtained from Gene Research Center (University of Tsukuba, Ibaraki, Japan).

Seedling were grown in Jiffy peat pots (Jiffy products international AS, Norway) in a growth chamber maintained under 16 h of light (150 $\mu\text{mol m}^{-2} \text{s}^{-1}$) at 24°C and 8 h of dark at 18°C and 60% humidity. Three-to four-week-old plants were sampled for morphological analysis.

2. Analysis of trichome morphology

A dissecting microscope (Leica M205A, Wetzlar, Germany) equipped with LED5000 RL light sources (Leica, Wetzlar, Germany) and a Leica MC170 HD Camera (Leica, Wetzlar, Germany) was used to analyze trichome morphology, size, and density. The images were analyzed with Photoshop Imaging Suite.

To examine trichome morphology in detail, Scanning Electron Microscopy (SEM) was performed using a Tabletop Microscope TM3030plus (Hitachi High-Technologies Corporation, Tokyo, Japan). The images were captured using 5kV to minimize surface charging of the trichomes. The images were analyzed with TM3030plus application software (ver. 01-05-02) and assembled with Photoshop Imaging Suite. All measurements were performed on WT and *hl5* plants grown side-by-side in the same growth chamber.

3. RT-PCR and genomic DNA PCR

Ribonucleic acid (RNA) extracted from leaves (TRIzol Reagent, Thermo Fisher Scientific) was used for complementary deoxyribonucleic acid (cDNA) synthesis (Thermoscript RT-PCR system, Invitrogen) according to the manufacturer's instructions. Full-length cDNAs corresponding to tomato actin related protein (ARP2/3)-WAVE complex genes were amplified by polymerase chain reaction (PCR) (T100 thermal cycler, BioRad). All primer sets used for reverse transcription (RT)-PCR are listed in Table 2. A cDNA encoding Actin was PCR-amplified using the Actin primer set (Table 2) and used as a loading control. RT-PCR (20 μ L) contained 2 μ L cDNA template, 1 μ L of a 10 μ M solution of each primer, 10 μ L Solg™ 2X Taq PCR Smart mix 2 (#SEF02, Solgent, Daejeon, Korea). The amplification protocol included an initial 2 min denaturation step at 95°C, followed by 35 cycles in which the template was denatured for 20 s at 95°C, annealed for 40 s at 60°C, and extended for 2~6 min at 72°C depending on expected cDNA length, followed by a final incubation for 5 min at 72°C. Amplified DNA products were separated on a 1% agarose gel.

Genomic DNA fragments corresponding to *SLARPCI* from WT and *hl5 plant* were PCR-amplified using the primer set listed in Table 2. PCR reactions (20 μ L) contained 2 μ L gDNA template, 1 μ L of a 10 μ M solution of each primer, 10 μ L Solg™ 2X Taq PCR Smart mix 2 (#SEF02, Solgent, Daejeon, Korea). Amplicons were produced by an initial 2min denaturation step at 95°C, followed by 35 cycles in which the template was denatured for 20 s at 95°C, annealed for 40 s at 60°C, and extended for 2 min at 72°C, followed by a final incubation for 5 min at 72°C. Amplified products were separated on a 1% agarose gel. Automated nucleotide sequencing was performed at Cosmogenetech (Seoul, Korea).

4. Amino acid alignment and phylogenetic analysis

ARPC1 amino acid sequences from *S. lycopersicum* SlARPC1 (Solyc05g006470), *A. thaliana* AtARPC1A (NP_180648.1), *A. thaliana* AtARPC1B (NP_180688.1), *S. tuberosum* StARPC1A1B (XP_006357213.1), *N. tabacum* NtARPC1A (XP_016461293.1), *O. sativa* OsARPC1B (XP_015623093), *D. melanogaster* DmARPC1A1B (NP_476596.1), *B. Taurus* BtARPC1A (NP_001068827.1), *B. Taurus* BtARPC1B (NP_001014844.1), *C. elegans* CeARPC1A1B (NP_499570.1) and *S. cerevisiae* ScARPC1A1B (NP_009793.1) were aligned using CLUSTALW. In CLUSTALW, the gap-opening and gap-extension penalties were set at 10 and 0.1, respectively, and the alignment was refined by using color align conservation (<http://www.bioinformatics.org/sms2/index.html>). The phylogenetic tree was constructed with the Maximum Likelihood method based on the JTT matrix-based model in MEGA7.

5. Vector construct

RNA was extracted from Micro-Tom (LA3911) tomato leaf using TRIZOL (Sigma-aldrich, 15596018, St.Louis, USA). The full length of *ARPC1* fragment was amplified from cDNA using Solg™ 2X Taq PCR Smart mix 2 (#SEF02, Solgent, Daejeon, Korea) with 5'- CGGATCCATGGCAGCAACTTCAGTACACAA -3' and 5'- CCGCTCGAGTCATAGATAGTCCAATAAATCTTCTTGTGTTTCTGCAA -3' primer set. PCR product was purified using a gel extraction kit (Cosmogenetech, CMA0112, Seoul, Korea). A pGEM-T plasmid containing a cDNA for the entire coding region of *SlARPC1* was reamplified with the ARPC1-BX primer set (Table 2). The resulting fragment was digested with *BamH* I (NEB, #R3136S, Ipswich, USA) and *Xho* I (NEB, #R0146S, Ipswich, USA) restriction enzymes to release a 1.1-kb

fragment. This product was cloned into *BamH* I and *Xho* I sites of the pBI-Tony binary vector, which contains the Cauliflower Mosaic Virus (CaMV) 35S promoter and the nopaline synthase (NOS) terminal, to generate pTony-35S::*ARPCI*. The *ARPCI* promoter region (approximately 4.5kb) was amplified by PCR (T100 thermal cycler, BioRad) using the ARPC1-SB primer set (Supplemental Table S0). The resulting fragment was digested with *Sbf*I and *Xba*I and cloned into the *Sbf*I and *Xba*I sites of pBI-Tony-35S::*ARPCI* to replace 35S promoter.

6. Tomato transformation

Cotyledons were used for transformation when there were no or minimal true leaves present on seedlings. Cotyledons were cut into four pieces and tips and bases were discarded. Middle parts of cotyledons were placed upside up on MS medium containing 2mg/L Zeatin, 0.1M acetosyringone (MS-Z) with a sterile filter paper for 2 days in a growth chamber at 25 °C, under 16h of light (50µmol m⁻²s⁻¹), 8h of dark and 60% humidity. Two days before co-cultivation, the *A. tumefaciens* strain LBA4404 containing the construct of *ARPCI* were streaked onto LB agar medium supplemented with 100mg/L Streptomycin, 50mg/L Rifampicin, 50mg/L Kanamycin. The plates were incubated for 36~48 h at 28 °C until colonies have developed. Colonies were selected from the plate and transferred to 30mL MS liquid medium and diluted to OD₆₀₀ value of 0.5. 0.1M acetosyringone was added to the final concentration of 100µM. The *A. tumefaciens* strain LBA4404 with vector construct culture was grown in a 250ml flask for 2 h at 28 °C, 200rpm. 10ml of acetosyringone treated *Agrobacterium* culture was pipetted over the pre-incubated cotyledons and incubated for 10 min. The explants placed upside up on new MS-Z plate with sterile filter paper and co-cultivated for 2 days in a 25 °C growth chamber. After two days of co-cultivation, the explants were rinsed in sterile water with 100mg/L Carbenicillin. The sterilized explants were transferred onto MS media containing 2mg/L Zeatin, 500mg/L Carbenicillin, 50mg/L Kanamycin. The plates were incubated in the 25 °C

growth chamber for 10 days. On day 10, cotyledons were transferred to new media plates. Thereafter explants were transferred at intervals of two weeks. Grown callus were transferred to MS media including 1mg/L Zeatin, 500mg/L Carbenicillin, 100mg/L Kanamycin. Thereafter grown shoots were cut off from explants and placed in MS media including 250mg/L Carbenicillin, 100mg/L Kanamycin.

7. Transgenic plants for complementary test

The resulting construct was introduced into *Agrobacterium tumefaciens* strain LBA4404 and used to transform *hl5* cotyledon explants. . The presence of the Transfer deoxyribonucleic acid T-DNA insert in independent primary (T_0) transformants was confirmed by PCR using the *35S::ARPC1* primer set (Table 2) to amplify a fragment spanning the CaMV promoter and *ARPC1* cDNA. The resulting construct (pBI-Tony-*ARPC1::ARPC1*) was introduced into *Agrobacterium tumefaciens* strain LBA4404 and used to transform *hl5* cotyledon explants. The presence of the T-DNA insert in independent primary (T_0) transformants was confirmed by PCR using the *ARPC1::ARPC1* primer set (Table 2) to amplify a fragment spanning the natural promoter and *ARPC1* cDNA. Regenerated T_0 transgenic plants containing the *ARPC1* transgene were potted in soil and transferred to a growth chamber for preliminary analysis of trichome morphology. These plants were subsequently transferred to a greenhouse for collection of seed (T_1 generation) from individual lines.

Results

1. Screening of Micro-Tom mutants related to trichome development

To study genes involved in trichome development in tomato, we screened Micro-Tom mutant population generated by Ethylmethane sulfonate (EMS) mutagenesis and selected four mutant lines showing abnormal trichome structure compared with wild-type (WT) plants. The images of dissecting microscopy showed that these four mutants have defects in trichome structure in leaves and stems (Figure 1), similar to previously known tomato trichome mutants *hairless (hl)* and *inquieta (ini)* which have swollen and distorted trichomes (Kang et al. 2010a; Jeong et al. 2017). So we designated the new mutants as *hl2*, *hl3*, *hl4*, and *hl5*.

2. RT-PCR analysis of tomato homologs of the ARP2/3-WAVE complex in *hl2*, *hl3*, *hl4*, and *hl5* mutants

Previous studies demonstrated that *Hl* and *Ini* encode SRA1 and ARPC2A, respectively, which are subunits of actin-related protein (ARP)2/3 and WAVE complexes involved in actin cytoskeleton formation (Kang et al. 2016; Jeong et al. 2017). In addition, Arabidopsis mutants defected in ARP2/3 or WAVE complex genes showed abnormally distorted trichomes (Basu et al. 2004; El-Assal et al. 2004; Szymanski 2005). So we hypothesized that the new four mutants are also defected in ARP2/3 or WAVE complex genes important for actin cytoskeleton formation. To test this hypothesis, we identified putative tomato homologs of the known subunits of the Arabidopsis ARP2/3 and WAVE complexes (Szymanski 2005; Jeong et al. 2017,

Table 1). Arabidopsis has 9 genes for ARP2/3 and 5 genes for WAVE complex. Tomato also has all homologs found in Arabidopsis. In Arabidopsis, *ARP3*, *ARPC3*, and *SCAR2* genes are single genes. However, tomato homologs of these genes are found to be two genes. In contrast, Arabidopsis *ARPC1A* and *ARPC1B* are found to be the same gene in tomato (Table 1). So we predicted that tomato has 10 genes for ARP2/3 and 6 genes for WAVE complex.

We used the full-length cDNA of the 16 homologs of ARP2/3-WAVE complex genes for RT-PCR to compare the expression pattern between the four mutants and WT plants. Among the 16 homologs, *Solyc02g014540* and *Solyc03g043720* were not amplified in WT (data not shown). The expression pattern of other 14 genes except *Solyc05g006470* was similar between the mutants and WT plants. The PCR fragment size of *hl5 Solyc05g006470* was slightly small compared with WT *Solyc05g006470* (Figure 2).

3. *hl5* affects trichome development

As observed with light microscopy, the morphology of trichomes on leaves, stems, hypocotyls, and sepals of the *hl5* mutant was significantly different from wild-type parent (cv Micro-Tom). The most obvious *hl5* phenotypes were the appearance of highly twisted and swollen trichomes (Figure 3). The identity of the distorted structures of *hl5* as type I trichomes was confirmed by scanning electron microscopy (SEM). The SEM analysis showed that type I trichomes on the *hl5* mutant contain highly swollen cells that fail to orient perpendicular to the leaf surface, resulting highly distorted and twisted structures (Figure 4). Other types of trichomes on the *hl5* mutant also showed swollen and distorted structures. Especially, the type VI trichome, which contains a short neck cell that connects the four-celled glandular head to the stem, showed irregular patterns of cell division on the *hl5* mutant. The neck cell of type VI trichomes on the *hl5* mutant also protruded from the side of the

stem, resulting in a glandular head that appeared to lay down on the leaf surface. Similar defects in trichome morphology were observed on *hl5* stems, hypocotyls, and sepals. SEM studies also showed that *hl5* affects the morphology of type V and VII trichomes. The size and shape of epidermal pavement cells on *hl5* leaves appeared normal. Previously we reported that aerial tissues of the tomato *hl* and *ini* mutants have swollen and distorted trichomes (Kang et al. 2010a, Jeong et al. 2017). Comparison of the *hl5* with *hl* and *ini* mutants showed that their distorted trichome phenotypes are strikingly similar (Figure 3 and Figure 4), suggesting that the *hl5*, *hl*, and *ini* mutations affect similar developmental processes.

4. *HL5* encodes the tomato homolog of ARPC1

In previous reverse transcription (RT)-PCR analysis (Figure 2), we found that *Solyc05g006470* showed a difference in size between *hl5* and wild-type plants. Based on this result, second RT-PCR analysis was performed for more accuracy. The result confirmed that there was a size difference in *hl5* compared to wild-type plant (Figure 5A). Full-length sequencing of cDNA of *Solyc05g006470* in WT and *hl5* plants showed that the entire exon 9 (82 bp) was deleted from *hl5* mutant (Figure 6). This polymorphism generates a premature stop codon that truncates the C-terminal 176 amino acids of the protein (Figure 7).

To investigate how exon skipping was induced from the *Solyc05g06470*, we performed PCR using genomic DNA in the range containing the deleted region of exon 9 from the cDNA sequencing results. The result showed that there was no significant size difference between *hl5* and wild-type plants (Figure 5B). Sequencing of these genomic DNA PCR fragments showed that single nucleotide substitution of G to A occurred in *hl5 Solyc05g06470* (Figure 5C and Figure 8). This alteration leads to a 5' splice-donor site mutation in intron 9, resulting in skipping of exon 9

(Figure 5C). These collective results demonstrate that the *hl5* mutant harbors a deletion in the *ARPC1* gene.

5. Comparison of ARPC1 homologs between tomato and other species

The *ARPC1* is predicted to encode for a 375-amino-acid protein. The ARPC1 homologs from a wide array of species (Figure 9A) share between 34 and 99% amino acid identity with ARPC1 from *S. lycopersicum*. In ARP2/3 complex, intersubunit contacts of ARPC1 with ARPC4 and ARPC5 are essential for activating and repressing ARP2/3 complex-mediated actin nucleation, respectively. Further, ARPC1 extended arm domain binds to that WASp VCA domain that mutations disrupting this interaction severely impair actin nucleation and are lethal in *S. cerevisiae* (Balcer, Daugherty-Clarke and Goode, 2010). According to this report, we speculate that disrupted interaction between ARPC1, ARPC4, ARPC5, and VCA domain in the *hl5* mutant may impair actin filament nucleation to give rise the irregular trichome morphology.

Phylogenetic analysis showed that plant ARPC1s cluster as a distinct phylogenetic clade relative to ARPC1 in yeast and animals (Figure 9B).

6. Genetic complementation of the *hl5* mutant restores normal trichome development

To verify whether the mutation in *ARPC1* causes the distorted trichome phenotype of *hl5* mutants, *Agrobacterium*-mediated transformation was used to complement the mutant with a cDNA that specifies the entire WT *ARPC1* coding region under the control of the 35S promoter of *Cauliflower Mosaic Virus* (CaMV) or the *ARPC1* natural promoter in the genetic background of the *hl5* mutant (Figure 10A). For the transformation we used BC₁F₃ plants from the cross between *hl5* and the Micro-Tom

wild-type. We obtained eight independent lines. In all transgenic plants, normal trichomes were shown on leaves, stems, and hypocotyls (Figure 10B).

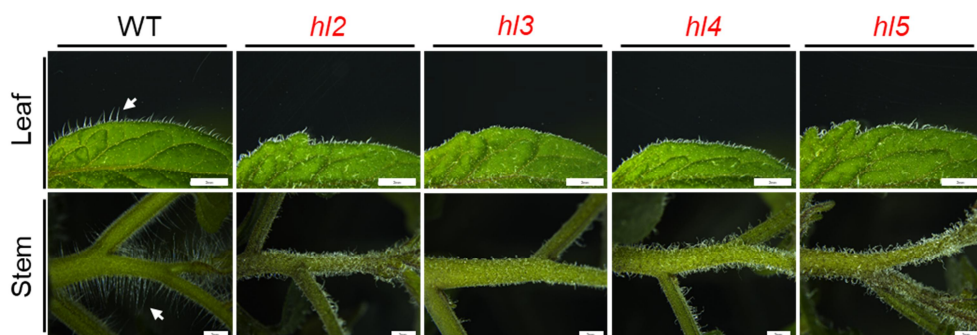


Figure 1. Light micrographs of trichomes in wild-type (WT) and distorted mutants. Photographs show the adaxial leaf surface (first row), stem (second row) of WT and distorted mutants (*hl2*, *hl3*, *hl4*, and *hl5*). The arrows indicate representative type I trichomes. All scale bars represent 2mm.

Gene name	Locus	WT	<i>hl2</i>	<i>hl3</i>	<i>hl4</i>	<i>hl5</i>
<i>ACTIN</i>	<i>Solyc03g078400</i>					
<i>ARP2</i>	<i>Solyc02g094320</i>					
<i>ARP3</i>	<i>Solyc05g013940</i>					
	<i>Solyc04g024530</i>					
<i>ARPC1</i>	<i>Solyc05g006470</i>					
<i>ARPC2A</i>	<i>Solyc11g068610</i>					
<i>ARPC2B</i>	<i>Solyc09g090550</i>					
<i>ARPC3</i>	<i>Solyc07g007630</i>					
<i>ARPC4</i>	<i>Solyc12g098430</i>					
<i>ARPC5A</i>	<i>Solyc01g090450</i>					
<i>NAP1</i>	<i>Solyc02g068720</i>					
<i>SRA1</i>	<i>Solyc11g013280</i>					
	<i>Solyc09g014980</i>					
<i>SCAR2</i>	<i>Solyc02g076840</i>					
	<i>Solyc02g076840</i>					
<i>ABI1L1</i>	<i>Solyc01g095280</i>					

Figure 2. RT-PCR analysis on the 14 tomato homologs of the ARP2/3-WAVE complex genes. RT-PCR was performed with *ACTIN* reference gene primers and the specific primers for *ARP2* (*Solyc02g094320*), *ARP3* (*Solyc05g013940*, *Solyc04g024530*), *ARPC1* (*Solyc05g006470*), *ARPC2A* (*Solyc11g068610*), *ARPC2B* (*Solyc09g090550*), *ARPC3* (*Solyc07g007630*), *ARPC4* (*Solyc12g098430*), *ARPC5A* (*Solyc01g090450*), *NAP1* (*Solyc02g068720*), *SRA1* (*Solyc11g013280*), *SCAR2* (*Solyc09g014980*, *Solyc02g076840*), *ABI1L1* (*Solyc01g095280*) gene expression in wild-type (WT), *hl2*, *hl3*, *hl4*, and *hl5* mutants. The *ACTIN* gene (*Solyc03g078400*) was

used as a control. All 14 tomato homologs of the ARP2/3-WAVE complex amplification reactions were carried out for 35 PCR cycles, and the *ACTIN* gene was amplified for 25 cycles.

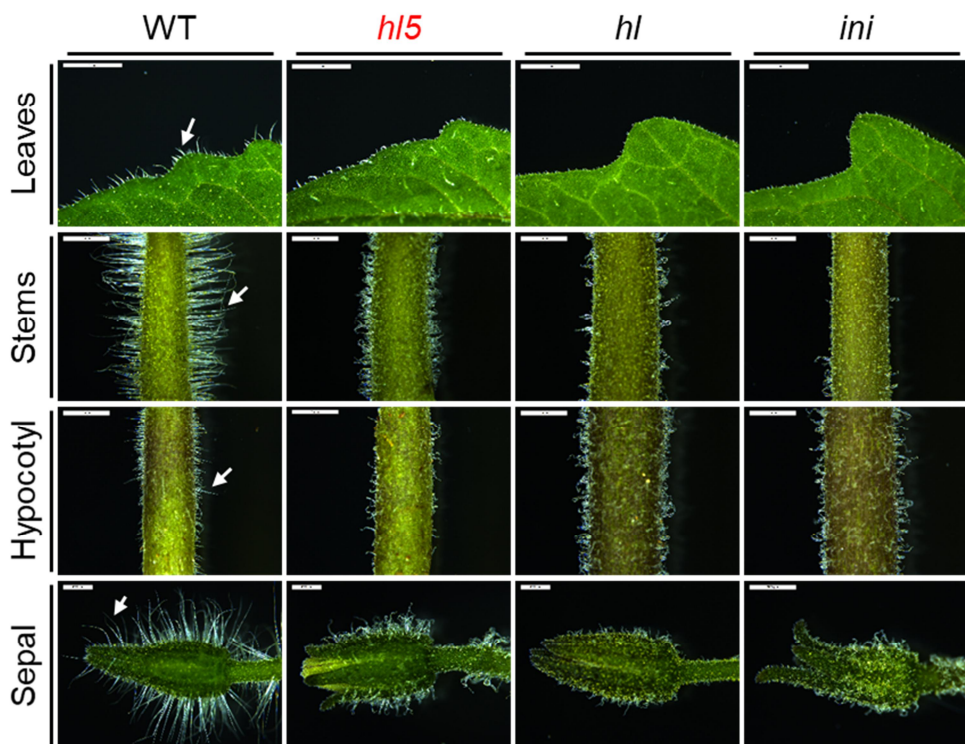


Figure 3. Light micrographs of trichomes on the leaf, stem, hypocotyl, and sepal of wild-type (WT), *hl5*, *hl*, and *ini* plants. Photographs show the adaxial leaf surface (first row), stem (second row), hypocotyl (third row), and sepal (forth row) of each genotype. Scale bars represent 1mm in the

leaves, stems, and hypocotyls, 500 μ m in the sepals. The arrows indicate type I trichomes.

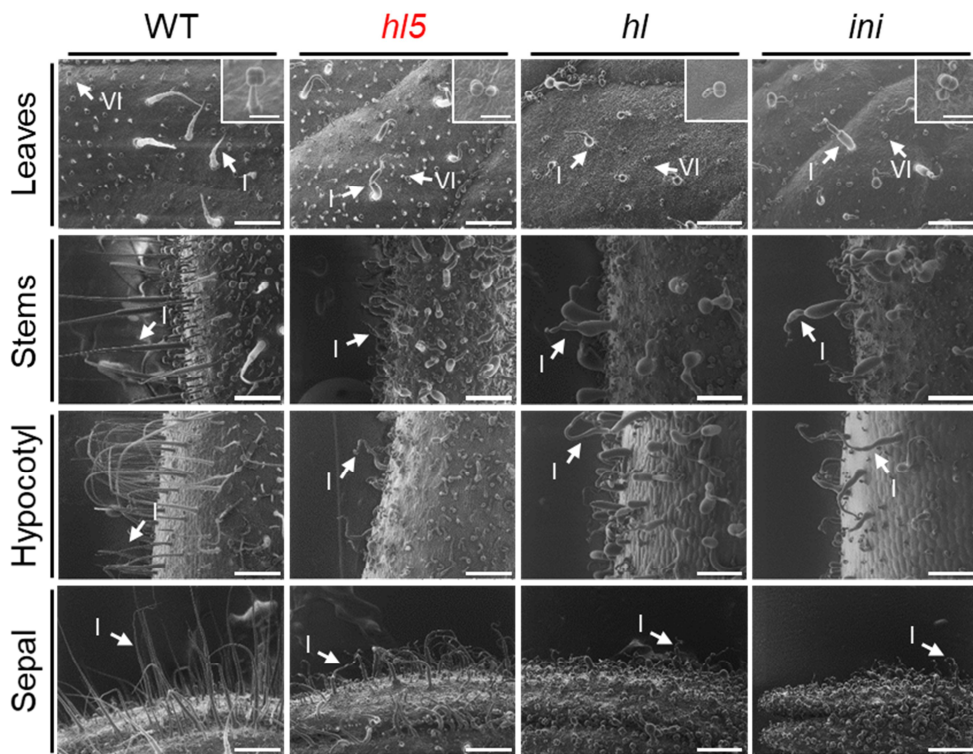


Figure 4. SEM micrographs of trichomes on the leaf, stem, hypocotyl, and sepal of wild-type (WT), *hl5*, *hl*, and *ini* plants. Photographs show the adaxial leaf surface (first row), stem (second row), hypocotyl (third row), and sepal (forth row) of each genotype. Scale bars represent 500 μ m in the leaves, stems, hypocotyls, and sepals, 100 μ m in the insets. Type I and VI trichomes

are indicated by arrows. Type VI trichomes marked by arrows are magnified in insets.

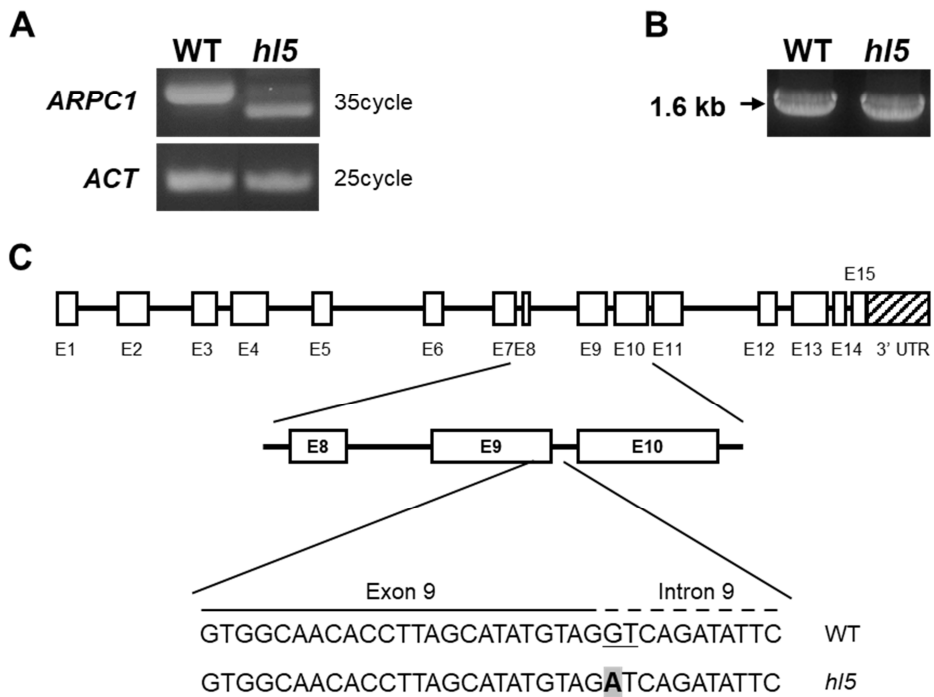


Figure 5. The *H15* gene encodes ARPC1.

(A) Agarose gel showing the results of RT-PCR amplification of *ARPC1* full-length cDNA using mRNA isolated from WT and *h15* plants. *ACTIN* (*Solyc03g078400*) gene was used as a loading control. (B) PCR amplification of partial length *ARPC1* genomic DNA from WT and *h15* plants. (C)

Schematic presentation for the splice site mutation in *hl5 ARPC1* gene. The splice-donor site in WT is underlined. The mutated single nucleotide sequence in *hl5* is highlighted with a box in gray color.

WT	ATGGCAGCAACTTCAGTACACAAGTTGCTCAGTGCAATTCTTGCCA TGCTTGGAGTCCCGACCTGTCCATGATTGCATT	80
<i>h15</i>	ATGGCAGCAACTTCAGTACACAAGTTGCTCAGTGCAATTCTTGCCA TGCTTGGAGTCCCGACCTGTCCATGATTGCATT	80

WT	CTGTCTAACACAGTGAAGTACATATTTATAAACTATCAGAAGACAAGTGGGAGAAGGCCATGTTCTTCAAAGCATG	160
<i>h15</i>	CTGTCTAACACAGTGAAGTACATATTTATAAACTATCAGAAGACAAGTGGGAGAAGGCCATGTTCTTCAAAGCATG	160

WT	ACCAAATGTTTCTGGTATCGATTGGAGTTACAGATCCAACA AAAATAGTCACTGTTTCTCATGACCGTAATTCATATGTC	240
<i>h15</i>	ACCAAATGTTTCTGGTATCGATTGGAGTTACAGATCCAACA AAAATAGTCACTGTTTCTCATGACCGTAATTCATATGTC	240

WT	TGGAACCAAGAAGCGACAGGTTGGGTTCTACCTGGTTATTCTCAGGCTGAATCGTGCAGCACTTTGTGTGCAGTGGAG	320
<i>h15</i>	TGGAACCAAGAAGCGACAGGTTGGGTTCTACCTGGTTATTCTCAGGCTGAATCGTGCAGCACTTTGTGTGCAGTGGAG	320

WT	TCCAAAAGAAAACAAGTTGCTGTGCGAAGTGGAGCTAAAAC TGTGTATATGCTACTACGAGCAAGAAAATAACTGGT	400
<i>h15</i>	TCCAAAAGAAAACAAGTTGCTGTGCGAAGTGGAGCTAAAAC TGTGTATATGCTACTACGAGCAAGAAAATAACTGGT	400

WT	GGGTGAGTAAGCTTATCAGGAAAAGACATGATTTCATCCGTAACAAGTATTGCCTGGCATCCAAAATAAGTCTTCTAGCA	480
<i>h15</i>	GGGTGAGTAAGCTTATCAGGAAAAGACATGATTTCATCCGTAACAAGTATTGCCTGGCATCCAAAATAAGTCTTCTAGCA	480

WT	ACAACGTCCACTGATGGTAAATGTAGAGTATTTTCAACATTCATTAAGGCGTCGATTCAAAGACTCTGCCATGGGAG	560
<i>h15</i>	ACAACGTCCACTGATGGTAAATGTAGAGTATTTTCAACATTCATTAAGGCGTCGATTCAAAGACTCTGCCATGGGAG	560

WT	TTCTGCAGATACCAAATTTGGAGGCAAAATGTTTCAGCTGATCTATGCTTTTGCTGGGCTTTGGTGTGCAGATGGTCCC	640
<i>h15</i>	TTCTGCAGATACCAAATTTGGAGG-----	585

WT	CAAGTGGCAACACCTTAGCATATGTAGGTCATAA CTCCATGATATACTTTGTTGATGAAGTGGTCCCTCTGCTGCAGCA	720
<i>h15</i>	-----GTCATAA CTCCATGATATACTTTGTTGATGAAGTGGTCCCTCTGCTGCAGCA	638

WT	CAAAGTGTAGCAATCCGTGATTTGCCTCTTCGTGATGTA TTGTTCTTCTGAAAGGATGGTGTGGAGTGGGATTTGA	800
<i>h15</i>	CAAAGTGTAGCAATCCGTGATTTGCCTCTTCGTGATGTA TTGTTCTTCTGAAAGGATGGTGTGGAGTGGGATTTGA	718

WT	TTGCAACCCGATGGTATTTGTGGCAGATGAAAGTGGACTCTGGAGTTCTTGAGATTCCTCGATGAACGGAAATCAGCGT	880
<i>h15</i>	TTGCAACCCGATGGTATTTGTGGCAGATGAAAGTGGACTCTGGAGTTCTTGAGATTCCTCGATGAACGGAAATCAGCGT	798

WT	CTTCAAGTGCCAAATATGGTGGATCACAGTTCGGAAGCATTTGGGAAATCTATGGTCAATCAAAGTTTCAGCCAGC	960
<i>h15</i>	CTTCAAGTGCCAAATATGGTGGATCACAGTTCGGAAGCATTTGGGAAATCTATGGTCAATCAAAGTTTCAGCCAGC	878

WT	AACAACGTTGAGCAGTCAAGAGGCGCTCATGACAACTGTATCAATTGCATATTACCACTTGCAAACAGAGAAAATCTAG	1040
<i>h15</i>	AACAACGTTGAGCAGTCAAGAGGCGCTCATGACAACTGTATCAATTGCATATTACCACTTGCAAACAGAGAAAATCTAG	958

WT	TGTCACCGTTTACCACCTTCAGGACTTGACGGGAAGATAGTGACATGGGATTTGCAGAAACAAGAAGTTATTGGACT	1120
<i>h15</i>	TGTCACCGTTTACCACCTTCAGGACTTGACGGGAAGATAGTGACATGGGATTTGCAGAAACAAGAAGTTATTGGACT	1038

WT	ATCTATGA	1128
<i>h15</i>	ATCTATGA	1046

Figure 6. Comparison of *ARPC1* cDNA sequence between wild-type (WT) and *hl5* plants. The regions highlighted with gray color represent exon9 (82bp) in WT *ARPC1* and deleted sequence region in *hl5 ARPC1*, respectively.

WT	MAATSVHKFAQCISCHAWSPDLSMIAFCPNNSEVHIYKLSSEDKWEKVHVLQKHDQIVSGI	60
<i>h15</i>	MAATSVHKFAQCISCHAWSPDLSMIAFCPNNSEVHIYKLSSEDKWEKVHVLQKHDQIVSGI	60

WT	DWSYRSNKIVTVSHDRNSYVWNQEATGWVPTLVILRLNRAALCVOWSPKENKFAVGSGAK	120
<i>h15</i>	DWSYRSNKIVTVSHDRNSYVWNQEATGWVPTLVILRLNRAALCVOWSPKENKFAVGSGAK	120

WT	TVCICYEEQENNNWVSKLIRKRHDSSVTSIAWHPNNVLLATTSTDGKCRVFSTFIKGVDS	180
<i>h15</i>	TVCICYEEQENNNWVSKLIRKRHDSSVTSIAWHPNNVLLATTSTDGKCRVFSTFIKGVDS	180

WT	KDSAMGSSADTKFGEQIVQLDLFCWAFGVRWSPSGNTLAYVGHNSMIYFVDEVGPSAAA	240
<i>h15</i>	KDSAMGSSADTKFGEVITP-----	199
	***** * ,	
WT	QSVAIRDLPLRDVLFLLSERMVGVGFDGNPMVVFVADESGLWSFLRFLDERKSASSSAKYG	300
<i>h15</i>	-----	
WT	GSQFSEAFGKFGQSKFSAENNVEQSRGAHDNCINCLPLAKQRKSSVTRFTTSGLDGKI	360
<i>h15</i>	-----	
WT	VTWDLQKQEDLLDYL	375
<i>h15</i>	-----	

Figure 7. Alignment of ARPC1 amino acid sequence from wild-type (WT) and *h15* plants.

WT	GAAAATCTTCATTGATGTTTTTTTTGTAAAAAAGAATTCTGGATAGCATTTCATATGTC	6989
<i>h15</i>	GAAAATCTTCATTGATGTTTTTTTTGTAAAAAAGAATTCTGGATAGCATTTCATATGTC	6989

WT	CTATTTTCATTATATGTCCATAGAAAGACTAATAGATCCTTTATTCATATTTAAATGCAG	7049
<i>h15</i>	CTATTTTCATTATATGTCCATAGAAAGACTAATAGATCCTTTATTCATATTTAAATGCAG	7049

WT	<u>CAAATTGTTTCAGCTTGATCTATGCTTTTGCTGGGCTTTGGTGTGATGGTCCCAAGT</u>	7109
<i>h15</i>	<u>CAAATTGTTTCAGCTTGATCTATGCTTTTGCTGGGCTTTGGTGTGATGGTCCCAAGT</u>	7109

WT	<u>GGCAACACCTTAGCATATGTAGATCAGATATTCCTTTCTTTGCTTCTTTGGCTTTTGCAT</u>	7169
<i>h15</i>	<u>GGCAACACCTTAGCATATGTAGATCAGATATTCCTTTCTTTGCTTCTTTGGCTTTTGCAT</u>	7169

WT	TATTTTAGCAGTGCCTCAACTGTCTCATTTTTGGTTGCATATTCGCATACTGTGTATGT	7229
<i>h15</i>	TATTTTAGCAGTGCCTCAACTGTCTCATTTTTGGTTGCATATTCGCATACTGTGTATGT	7229

WT	GTGTTCAATTGTGCAATTTTTATTTTTCTTGATCTTGACTAAGTACCCAGAATTTTGC	7289
<i>h15</i>	GTGTTCAATTGTGCAATTTTTATTTTTCTTGATCTTGACTAAGTACCCAGAATTTTGC	7289

WT	ATGTAATACTAATGCAGCTTAGATATTGGGTTTGGATGGTCTCTCAGGTCATAACTCCA	7349
<i>h15</i>	ATGTAATACTAATGCAGCTTAGATATTGGGTTTGGATGGTCTCTCAGGTCATAACTCCA	7349

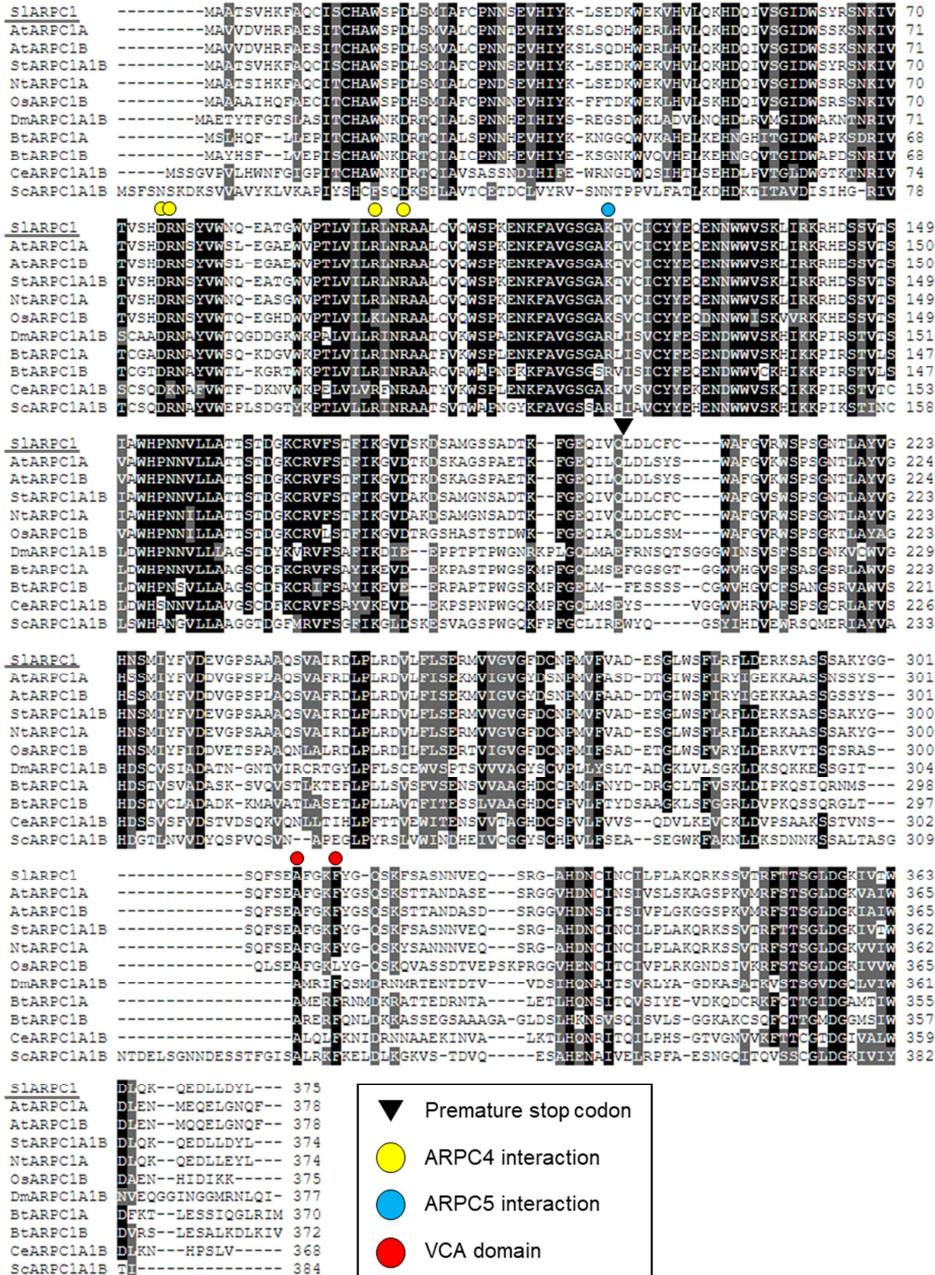
WT	<u>TGATATACTTTGTTGATGAAGTTGGTCCCTCTGCTGCAGCACAAAGTGTAGCAATCCGTG</u>	7409
<i>h15</i>	<u>TGATATACTTTGTTGATGAAGTTGGTCCCTCTGCTGCAGCACAAAGTGTAGCAATCCGTG</u>	7409

WT	<u>ATTTGCCTCTTCGTGATGTGGGTCAGAATCCTGTCTCATTTTACTTTGTCTATTTAGAC</u>	7469
<i>h15</i>	<u>ATTTGCCTCTTCGTGATGTGGGTCAGAATCCTGTCTCATTTTACTTTGTCTATTTAGAC</u>	7469

WT	CTTAATATTTGTTGTGTAATCAAGACTTCTCTTGCAG	7506
<i>h15</i>	CTTAATATTTGTTGTGTAATCAAGACTTCTCTTGCAG	7506

Figure 8. Comparison of *ARPC1* genomic DNA sequence between wild-type (WT) and *h15* plants. Exon9 and exon10 are indicated by underlines. The mutated single nucleotide sequence is highlighted with grey color in *h15* mutant.

A



B

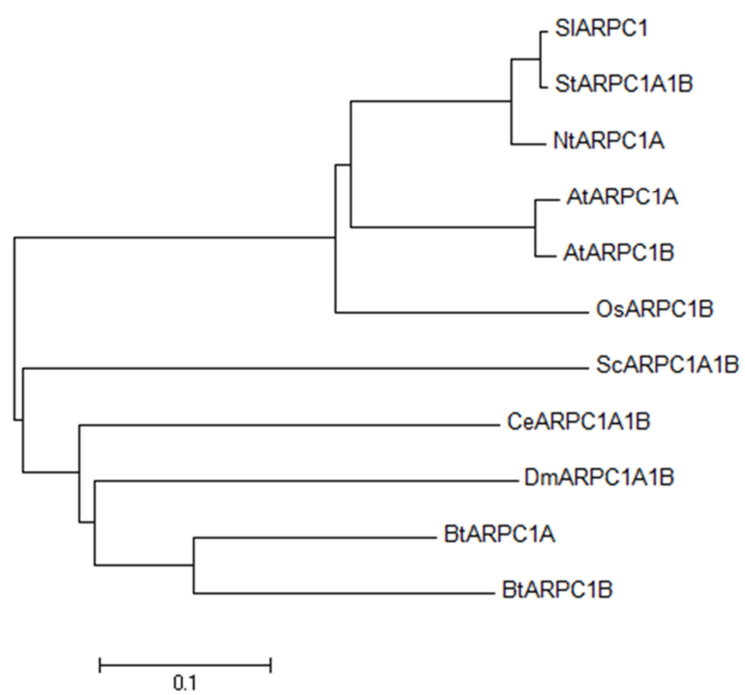


Figure 9. Similarity of ARPC1 between tomato and other species.

(A) Comparison of the predicted amino acid sequence of ARPC1 in tomato and other species. Amino acid residues in black indicate identity, and those in gray indicate conserved substitutions. The position of premature stop codon in *ARPC1* of *hl5* is marked by a black triangle. The critical amino acid residues for the interaction with ARPC4, ARPC5, and VCA domain in *S. cerevisiae* species are marked with yellow, blue, and red circles, respectively. *S. lycopersicum* SlARPC1 (Solyc05g006470), *A. thaliana* AtARPC1A (NP_180648.1), *A. thaliana* AtARPC1B (NP_180688.1), *S. tuberosum* StARPC1A1B (XP_006357213.1), *N. tabacum* NtARPC1A (XP_016461293.1), *O. sativa* OsARPC1B (XP_015623093), *D. melanogaster* DmARPC1A1B (NP_476596.1), *B. Taurus* BtARPC1A (NP_001068827.1), *B. Taurus* BtARPC1B (NP_001014844.1), *C. elegans* CeARPC1A1B (NP_499570.1) and *S. cerevisiae* ScARPC1A1B (NP_009793.1).

(B) Phylogenetic tree of ARPC1 in tomato and other species. The unrooted phylogenetic tree was constructed by the Maximum Likelihood method using MEGA7 with amino acid sequences of ARPC1 from nine different species. *S. lycopersicum* SlARPC1 (Solyc05g006470), *A. thaliana* AtARPC1A (NP_180648.1), *A. thaliana* AtARPC1B (NP_180688.1), *S. tuberosum* StARPC1A1B (XP_006357213.1), *N. tabacum* NtARPC1A (XP_016461293.1), *O. sativa* OsARPC1B (XP_015623093), *D. melanogaster* DmARPC1A1B (NP_476596.1), *B. Taurus* BtARPC1A

(NP_001068827.1), *B. Taurus* BtARPC1B (NP_001014844.1), *C. elegans* CeARPC1A1B (NP_499570.1) and *S. cerevisiae* ScARPC1A1B (NP_009793.1).

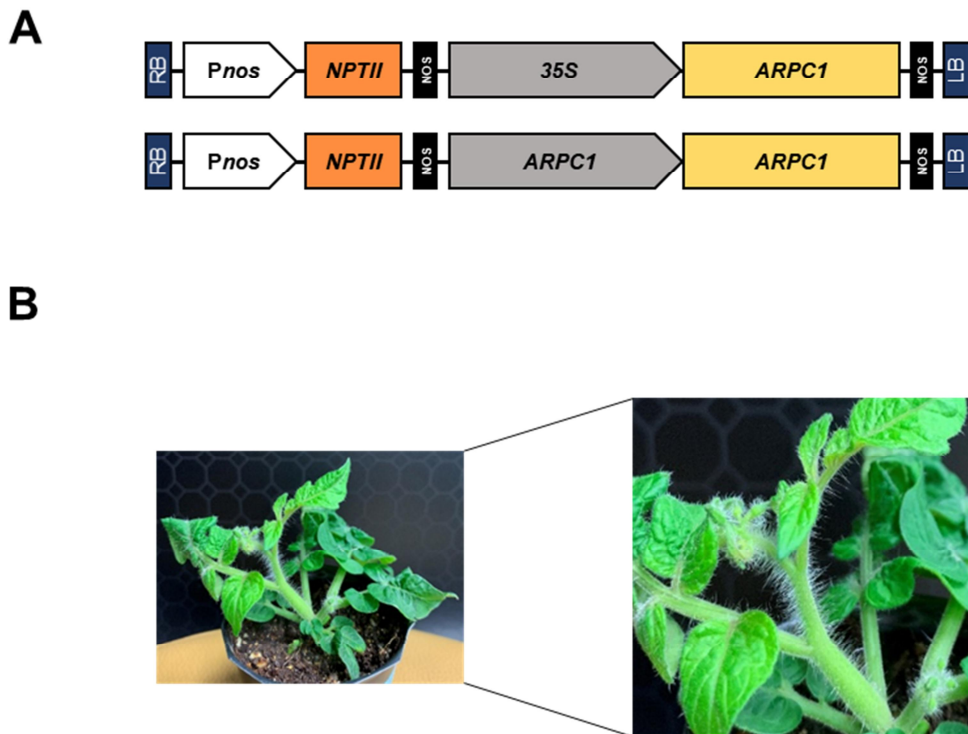


Figure 10. *ARPC1* complements the trichome morphology defect of the *hl5* mutant. (A) Schematic presentation of *35S::ARPC1* and *ARPC1::ARPC1* vectors. (B) Phenotype of *hl5* mutant plants complemented with *ARPC1::ARPC1* vector.

Arabidopsis			Tomato*			
Genetic name	Gene name	Locus code	Genetic name	Locus code*	E value†	Identity with Arabidopsis homolog (%)
<i>WURM</i>	<i>ARP2</i>	AT3G27000		<u>Solyc02g094320</u>	0	90
<i>DIS1</i>	<i>ARP3</i>	AT1G13180		<u>Solyc05g013940</u>	0	83
	<i>ARPC1A</i>	AT2G30910	<i>Hl5</i>	<u>Solyc04g024530</u>	0	82
	<i>ARPC1B</i>	AT2G31300		Solyc05g006470	0	76
<i>DIS2</i>	<i>ARPC2A</i>	AT1G30825	<i>Ini</i>	<u>Solyc11g068610</u>	1.00E-162	69
	<i>ARPC2B</i>	AT2G33385		<u>Solyc09g090550</u>	1.00E-136	52
	<i>ARPC3</i>	AT1G60430		<u>Solyc07g007630</u>	1.00E-111	86
	<i>ARPC4</i>	AT4G14147		<u>Solyc02g014540</u>	1.00E-60	73
<i>CRK</i>	<i>ARPC5A</i>	AT4G01710		<u>Solyc12g098430</u>	1.00E-113	92
<i>GRL</i>	<i>NAP1</i>	AT2G35110		<u>Solyc01g090450</u>	3.00E-82	86
<i>PIR/KLK</i>	<i>SRA1</i>	AT5G18410	<i>Hl</i>	<u>Solyc02g068720</u>	0	76
				<u>Solyc11g013280</u>	0	78
				<u>Solyc11g013290</u>	0	90
<i>BRK1</i>	<i>BRICK1</i>	AT2G22640		<u>Solyc03g043720</u>	2.00E-50	90
<i>DIS3</i>	<i>SCAR2</i>	AT2G38440		<u>Solyc09g014980</u>	1.00E-115	49
				<u>Solyc02g076840</u>	5.00E-59	51
	<i>ABI1L1</i>	AT2G46225		<u>Solyc01g095280</u>	1.00E-114	60

Table 1. Arabidopsis genes encoding subunits of the ARP2/3-WAVE complexes and their homolog genes in tomato. *: Tomato homologs of Arabidopsis ARP2/3-WAVE complex genes were identified by a blast search using tomato genome chromosomes (build SL2.5) in the Sol Genomics Network (<http://solgenomics.net/>). †: E value and identity were obtained by aligning each homolog in tomato and Arabidopsis using blastp in the National Center for Biotechnology Information (<http://www.ncbi.nlm.nih.gov/>). Tomato *Hairless* (*SRA1*) and *Ini* (*ARPC2A*) genes are underlined and *Hairless5* (*ARPC1*) gene is in bold, respectively.

Primer name	Primer sequence (5'→3')	Description
Actin	F:GGGATGGAGAAATTTGGTGGTGG R:CTTCGACCAAGGATGGTGTAGC	Control for RT-PCR
ARP2- <i>full</i>	F:ATGGATAATCGAAACGTTGTCTGT R:TCATGCCTGACCCACACTTCG	Amplifies full-length <i>Solyc02g004320</i> cDNA
ARP3-1- <i>full</i>	F:ATGATAATGGACCCCTGCTACCTCT R:TCAGTACATCCCTTAAATACAGGGTT	Amplifies full-length <i>Solyc05g013940</i> cDNA
ARP3-2- <i>full</i>	F:ATGGACCTTCTACCTCTCGC R:TCATACATTCCTTAAATACGGGA	Amplifies full-length <i>Solyc04g024530</i> cDNA
ARPC1A, 1B- <i>full</i>	F:ATGGCAGCAACTTCAGTACACA R:TCATAGATAGTCCAAATAAATCTTTGTTTCT	Amplifies full-length <i>Solyc05g006470</i> cDNA
ARPC2A- <i>full</i>	F:GCGGATCCCGATGATATTACTGCAATCTCCCTCTAG R:CACTCGAGTCTACTTCCAACTTCGGAAAC	Amplifies full-length <i>Solyc11g008010</i> cDNA
ARPC2B- <i>full</i>	F:ATGGCCGTTTTGAACG R:TTAATTGGTTGAAGAGAAATATCTTTTTCC	Amplifies full-length <i>Solyc09g090550</i> cDNA
ARPC3-1- <i>full</i>	F:ATGGTTTATCATTCAGTTTCGTTG R:TCAAGGAAGAACCATGTTTATAAACT	Amplifies full-length <i>Solyc07g007030</i> cDNA
ARPC3-2- <i>full</i>	F:ATGATTTGCCTAATACTAAATCCTCAAGG R:TCAGAACTTGCCTGGTTCGT	Amplifies full-length <i>Solyc02g014540</i> cDNA
ARPC4- <i>full</i>	F:ATGGCAAATCCGTTGCG R:TCAGATGAATTGGTTCAGAAACTCA	Amplifies full-length <i>Solyc12g008430</i> cDNA
ARPC5A- <i>full</i>	F:ATGGCTGAGATGTCGAAGCA R:TCACACAGTATTCACAGTGTACGCA	Amplifies full-length <i>Solyc01g090450</i> cDNA
NAP1- <i>full</i>	F:ATGACTAAACCGAGCGCAGCAG R:TCACCTTGAAGATATAGGCCGGATCT	Amplifies full-length <i>Solyc02g008720</i> cDNA
SRA1- <i>full</i>	F:TCAAATGGCGGTTCCGATTGAAGAA R:AGCAGCCTCAGGCACCTTCTGTGGC	Amplifies full-length <i>Solyc11g013200</i> cDNA
BRICK1- <i>full</i>	F:ATGCTTGCCCTTTGAAGAACAAAG R:TCAAACATTAACACAGAGCTGGATTAGC	Amplifies full-length <i>Solyc03g043720</i> cDNA
SCAR2-1- <i>full</i>	F:ATGGCTGGAATAGGTATCAGATTCC R:TTATGAATCCTCCAAAGAAATCCTCC	Amplifies full-length <i>Solyc09g014980</i> cDNA
SCAR2-2- <i>full</i>	F:ATGCCGTTGGTGAGAACTGC R:TCAGTGTCACTCCAGTTATCTTCC	Amplifies full-length <i>Solyc02g070840</i> cDNA
ABIHL1- <i>full</i>	F:ATGGAAATGAAACAAATGAAATGTTGG R:TTACGACACAGCACTGGTCTTC	Amplifies full-length <i>Solyc01g095280</i> cDNA
ARPC1-gDNA1	F:TTGGAACAGAGACTCTGCCATG R:CAACCAGAGTCCACTTTCATCTGC	Amplifies genomic region containing ARPC1 exon 8 to 11
ARPC1-BX	F:CGGATCCATGGCAGCAACTTCAGTACAAA R:CCGTCGAGTCATAGATGCCAAATAAATCTTCTGTTTCTGCAA	Used to clone ARPC1 into binary vector pBI-Tony with 35S promoter. Forward and reverse primers contain BamHI and XhoI site, respectively.
ARPC1-SB	F:GCCCTCAGGCAACACTCCATATTCATGGACTCATATGAG R:CGGATCCTGATTTGCCTACAAAATGATCTAAAAAATACGATTAGCAG	Used to clone ARPC1 into binary vector pBI-Tony with natural promoter. Forward and reverse primers contain SbfI and BamHI site, respectively.

Start and stop codon are in bold. Restriction enzyme sites are underlined. F, Forward primer ; R, Reverse primer

Table 2. Description of PCR primers used in this study

Discussion

The analysis on mutants related to trichome development in Arabidopsis has been effectual for interpreting the fundamental molecular mechanisms for the development of simple unicellular trichomes. The ‘distorted group’ (*dis*) of trichome morphology mutants has been studied to play an important role in actin filament nucleation and morphogenesis (Basu et al. 2004; Basu et al. 2005; Le et al. 2006). Molecular analysis of Arabidopsis *dis* genes encode subunits of two different complexes: the actin-related protein (ARP)2/3 complex that nucleates actin filaments and the WAVE complex that regulates the activity of ARP2/3. The ARP2/3 complex is a conserved seven-subunit actin nucleating machine (ARP2, ARP3, ARPC1, ARPC2, ARPC3, ARPC4, and ARPC5), and the WAVE complex contains five subunits (NAP1, SRA1, BRICK1, SCAR2, and ABI1L1) (Table 1) (Szymanski 2005; Robinson, 2001). Based on the similarity of phenotype (e.g. curled and distorted trichomes) between these mutants and the tomato mutants, we previously demonstrated that *Hl* and *Ini* genes are involved in the polymerization of actin cytoskeleton (Kang et al. 2016; Jeong et al. 2017). Here, we identified the *ARPC1* gene of *hl5* mutant and this result provide additional genetic evidence that a subunit of ARP2/3 complex is crucial for normal trichome development in tomato.

Most plant mRNAs are synthesized as precursors containing one or more introns that are removed during the process of splicing. The basic mechanism of spliceosome assembly and intron excision is similar in all eukaryotes. However, the recognition of introns in plants has some unique features, which distinguishes it from the reactions in vertebrates and yeast. Recent progress has occurred in characterizing the splicing signals in plant pre-mRNAs, in identifying the mutants affected in splicing and in discovering new examples of alternatively spliced mRNAs. In combination with information provided by the Arabidopsis genome-sequencing project, these studies are contributing to a better understanding of the splicing process and its role in the regulation of gene expression in plants. Two sequence structural features are required for correct pre-mRNA splicing: The first one is that the splice site sequences are present at the exon-intron borders. The splice sites consist of the 5' and the 3' splice sites, the former, designated as splice donor, the site includes a GU dinucleotide located on the exon/intron junction at the 5' end of the intron, and the latter called splice acceptor which locates at the another end of the intron containing three conserved sequence elements. In this study, we identified a *H15* gene. The difference between wild-type (WT) and *h15* mutant is a single base substitution of G to A of the intron 9. This mutation happened within the 5' splice site and destroyed the splice donor site from GU to AU, which led to a missplicing, resulting the entire exon 9 (82bp) was deleted from *h15* mutant. This polymorphism generates a premature stop codon that truncates the C-terminal 176 amino acids of the protein.

Our results demonstrated that the *h15* mutant harbors a deletion in the *ARPCI* gene and this deletion is associated with lack of detectable expression

of normal *ARPC1* transcripts in the mutant. In ARP2/3 complex, intersubunit contacts of ARPC1 with ARPC4 and ARPC5 are essential for activating and repressing ARP2/3 complex-mediated actin nucleation, respectively. Further, ARPC1 extended arm domain binds to that WASp VCA domain that mutations disrupting this interaction severely impair actin nucleation and are lethal in *S. cerevisiae* (Balcer, Daugherty-Clarke and Goode, 2010). According to this report, we speculate that disrupted interaction between ARPC1, ARPC4, ARPC5, and VCA domain in the *hl5* mutant may impair actin filament nucleation to give rise to the irregular trichome morphology. To prove this hypothesis, we tested functional complementation of the *hl5* mutant with the normal *ARPC1* gene. These showed that the defects in trichome morphology in the *hl5* mutant result from a defective *ARPC1* gene.

In addition to tomato and Arabidopsis, numerous studies have demonstrated that genes encoding subunits of the ARP2/3 and WAVE complexes in other plants are also important for epidermal cell morphogenesis. For example, a soybean *gnarled* trichome mutant is impaired in *NAP1* gene (Campbell et al. 2016). The rice mutants *less pronounced lobe epidermal cell (lpl)2* and *lpl3* that encode SRA1 and NAP1, respectively, show an epidermal cell defect (Zhou et al. 2016). The *arpc1* mutant in *Lotus japonicus* and the *required for infection thread (rit)* mutant encoding NAP1 in *Medicago truncatula* also show a trichome distortion phenotype (Hossain et al. 2012; Miyahara et al. 2010). The *arpc1* in *Physcomitrella patens* encoding ARPC1 show a defect in cell morphology manifested as short, irregularly shaped cells with abnormal division patterns (Harries, 2005). These collective data indicate that the function of ARP2/3-WAVE complex in epidermal cells development is evolutionarily conserved in plant species.

Several previous studies suggest that the function of ARP2/3 and WAVE complexes is not limited to trichome development. For example, Arabidopsis ARP2, ARP3, and ARPC2 play an important role in stomatal movement by reorganizing actin filaments and vacuoles in guard cells (Jiang et al. 2012; Li et al. 2013). Arabidopsis ARP2 regulates mitochondrial-dependent calcium signaling in response to salt stress (Zhao et al. 2013). Arabidopsis NAP1 acts as a regulator of autophagy in response to nitrogen starvation and salt stress (Wang et al. 2016). The Arabidopsis ARP2/3 and WAVE complexes also regulate light-induced root elongation by controlling the expression of longitudinal F-actin through photoreceptors and the 26S proteasome (Dyachok et al. 2011). In rice, the *early senescence1* mutant encoding SCAR-LIKE PROTEIN2 exhibits higher stomatal density, resulting in excessive water loss (Rao et al. 2015). The tomato *Hl* gene encoding SRA1 is involved in the production of terpenoids and flavonoids (Kang et al. 2016). The tomato *Ini* gene encoding ARPC2A is associated with regulating actin cytoskeleton formation (Jeong et al. 2017). The ARP2/3-WAVE complex is also required for rhizobial infection of root hair in leguminous plants such as *Lotus japonicus* and *Medicago truncatula* (Hossain et al. 2012; Gavrin et al. 2015; Miyahara et al. 2010; Qiu et al. 2015). In addition, the stomatal response to darkness is mediated by reorganisation of guard cell actin filaments, a process that is finely tuned by the conserved SCAR/WAVE-ARP2/3 actin regulatory module (Isner et al. 2017). The tomato *hl5* mutant described here would provide a useful tool to further unravel the diverse functions of the actin cytoskeleton in plants.

References

Balcer, H., Daugherty-Clarke, K. and Goode, B. (2010) The p40/ARPC1 Subunit of Arp2/3 Complex Performs Multiple Essential Roles in WASp-regulated Actin Nucleation. *Journal of Biological Chemistry*, 285(11), pp.8481-8491.

Basu D, El-Assal SED, Le J, Mallery EL, Szymanski DB (2004) Interchangeable functions of *Arabidopsis* PIROGI and the human WAVE complex subunit SRA1 during leaf epidermal development. *Development* **131**:4345-4355

Bleeker PM, Mirabella R, Diergaarde PJ, VanDoorn A, Tissier A, Kant MR, Prins M, de Vos M, Haring MA, Schuurink RC (2012) Improved herbivore resistance in cultivated tomato with the sesquiterpene biosynthetic pathway from a wild relative. *P Natl Acad Sci* **109**:20124-20129

Campbell BW, Hofstad AN, Sreekanta S, Fu F, Kono TJY, O'Rourke JA, Vance CP, Muehlbauer GJ, Stupar RM (2016) Fast neutron-induced structural rearrangements at a soybean *NAPI* locus result in *gnarled* trichomes. *Theor Appl Genet* **129**:1725-1738

Dyachok J, Zhu L, Liao FQ, He J, Huq E, Blancaflor EB (2011) SCAR mediates light-induced root elongation in *Arabidopsis* through photoreceptors and proteasomes. *Plant Cell* **23**:3610-3626

Ehleringer JR, Mooney HA (1978) Leaf hairs: Effects on physiological activity and adaptive value to a desert shrub. *Oecologia* **37**:183-200

El-Assal SE, Le J, Basu D, Mallery EL, Szymanski DB (2004) DISTORTED2 encodes an ARPC2 subunit of the putative *Arabidopsis* ARP2/3 complex. *Plant J* **38**:526-538

Gan YB, Kumimoto R, Liu C, Ratcliffe O, Yu H, Broun P (2006) GLABROUS INFLORESCENCE STEMS modulates the regulation by gibberellins of epidermal differentiation and shoot maturation in *Arabidopsis*. *Plant Cell* **18**:1383-1395

Gavrin A, Jansen V, Ivanov S, Bisseling T, Fedorova E (2015) ARP2/3-mediated actin nucleation associated with symbiosome membrane is essential for the development of symbiosomes in infected cells of *Medicago truncatula* root nodules. *Mol Plant Microbe In* **28**:605-614

Goffreda JC, Steffens JC, Mutschler MA (1990) Association of epicuticular sugars with aphid resistance in hybrids with wild Tomato. *J Am Soc Hortic Sci* **115**:161-165

Goffreda JC, Steffens JC, Mutschler MA (1990) Association of epicuticular sugars with aphid resistance in hybrids with wild Tomato. *J Am Soc Hortic Sci* **115**:161-165

Grebe M (2012) The patterning of epidermal hairs in *Arabidopsis* - updated. *Curr Opin Plant Biol* **15**:31-37

Harries, P. (2005) Actin-Related Protein2/3 Complex Component ARPC1 Is Required for Proper Cell Morphogenesis and Polarized Cell Growth in *Physcomitrella patens*. *THE PLANT CELL ONLINE*, 17(8), pp.2327-2339.

Hossain, M., Liao, J., James, E., Sato, S., Tabata, S., Jurkiewicz, A., Madsen, L., Stougaard, J., Ross, L. and Szczygłowski, K. (2012) Lotus japonicus ARPC1 Is Required for Rhizobial Infection. *PLANT PHYSIOLOGY*, 160(2), pp.917-928.

Isner, J., Xu, Z., Costa, J., Monnet, F., Batstone, T., Ou, X., Deeks, M., Genty, B., Jiang, K. and Hetherington, A. (2017) Actin filament reorganisation controlled by the SCAR/WAVE complex mediates stomatal response to darkness. *New Phytologist*, 215(3), pp.1059-1067.

Jeong, N., Kim, H., Hwang, I., Howe, G. and Kang, J. (2017) Genetic analysis of the tomato *inquieta* mutant links the ARP2/3 complex to trichome development. *Journal of Plant Biology*, 60(6), pp.582-592.

Jiang K, Sorefan K, Deeks MJ, Bevan M, Hussey PJ, Hetherington AM (2012) The ARP2/3 Complex mediates guard cell actin reorganization and stomatal movement in *Arabidopsis*. *Plant Cell* **24**:2031-2040

Juvik JA, Shapiro JA, Young TE, Mutschler MA (1994) Acylglucosides from wild tomatoes alter behavior and reduce growth and survival of *Helicoverpa zea* and *Spodoptera exigua* (Lepidoptera, Noctuidae). *J Econ Entomol* **87**:482-492

Kang JH, Campos ML, Zemelis-Durfee S, Al-Haddad JM, Jones AD, Telewski FW, Brandizzi F, Howe GA (2016) Molecular cloning of the tomato *Hairless* gene implicates actin dynamics in trichome-mediated defense and mechanical properties of stem tissue. *J Exp Bot* **67**:5313-5324

Kang JH, Liu GH, Shi F, Jones AD, Beaudry RM, Howe GA (2010b) The tomato *odorless-2* mutant is defective in trichome-based production of diverse specialized metabolites and broad-spectrum resistance to insect herbivores. *Plant Physiol* **154**:262-272

Kang JH, McRoberts J, Shi F, Moreno JE, Jones AD, Howe GA (2014) The flavonoid biosynthetic enzyme chalcone isomerase modulates terpenoid production in glandular trichomes of tomato. *Plant Physiol* **164**:1161-1174

Kang JH, Shi F, Jones AD, Marks MD, Howe GA (2010a) Distortion of trichome morphology by the *hairless* mutation of tomato affects leaf surface chemistry. *J Exp Bot* **61**:1053-1064

Karabourniotis G, Papadopoulos K, Papamarkou M, Manetas Y (1992) Ultraviolet-B radiation absorbing capacity of leaf hairs. *Physiologia Plantarum* **86**:414-418

Kennedy GG (2003) Tomato, pests, parasitoids, and predators: tritrophic interactions involving the genus *Lycopersicon*. *Annu Rev Entomol* **48**:51-72

Le, J., Mallery, E., Zhang, C., Brankle, S. and Szymanski, D. (2006) Arabidopsis BRICK1/HSPC300 Is an Essential WAVE-Complex Subunit that Selectively Stabilizes the Arp2/3 Activator SCAR2. *Current Biology*, 16(9), pp.895-901.

Li LJ, Ren F, Gao XQ, Wei PC, Wang XC (2013) The reorganization of actin filaments is required for vacuolar fusion of guard cells during stomatal opening in *Arabidopsis*. *Plant Cell Environ* **36**:484-497

Luckwill LC (1943) The genus *Lycopersicon*: a historical, biological and taxonomic survey of the wild and cultivated tomatoes. UK: University of Aberdeen

Miyahara A, Richens J, Starker C, Morieri G, Smith L, Long S, Downie JA, Oldroyd GED (2010) Conservation in function of a SCAR/WAVE component during infection thread and root hair growth in *Medicago truncatula*. *Mol Plant Microbe In* **23**:1553-1562

Oppenheimer DG, Pollock MA, Vacik J, Szymanski DB, Ericson B, Feldmann K, Marks MD (1997) Essential role of a kinesin-like protein in *Arabidopsis* trichome morphogenesis. *P Natl Acad Sci* **94**:6261-6266

Qiu LP, Lin JS, Xu J, Sato S, Parniske M, Wang TL, Downie JA, Xie F (2015) SCARN a novel class of SCAR protein that is required for root-hair infection during legume nodulation. *PLoS Genet* **11**:

Ramsay, N. and Glover, B. (2005) MYB–bHLH–WD40 protein complex and the evolution of cellular diversity. *Trends in Plant Science*, 10(2), pp.63-70.

Rao, Y., Yang, Y., Xu, J., Li, X., Leng, Y., Dai, L., Huang, L., Shao, G., Ren, D., Hu, J., Guo, L., Pan, J. and Zeng, D. (2015) EARLY SENESCENCE1 Encodes a SCAR-LIKE PROTEIN2 That Affects Water Loss in Rice. *Plant Physiology*, 169(2), pp.1225-1239.

Robinson, R. (2001) Crystal Structure of Arp2/3 Complex. *Science*, 294(5547), pp.1679-1684.

Rodriguez AE, Tingey WM, Mutschler MA (1993) Acylsugars of *Lycopersicon pennellii* deter settling and feeding of the green peach Aphid (Homoptera, Aphididae). *J Econ Entomol* **86**:34-39

Sallaud C, Rontein D, Onillon S, Jabes F, Duffe P, Giacalone C, Thoraval S, Escoffier C, Herbette G, Leonhardt N, Causse M, Tissier A (2009) A novel

pathway for sesquiterpene biosynthesis from Z,Z-Farnesyl Pyrophosphate in the wild tomato *Solanum habrochaites*. *Plant Cell* **21**:301-317

Schillmiller AL, Charbonneau AL, Last RL (2012) Identification of a BAHD acetyltransferase that produces protective acyl sugars in tomato trichomes. *P Natl Acad Sci* **109**:16377-16382

Schillmiller AL, Schauvinhold I, Larson M, Xu R, Charbonneau AL, Schmidt A, Wilkerson C, Last RL, Pichersky E (2009) Monoterpenes in the glandular trichomes of tomato are synthesized from a neryl diphosphate precursor rather than geranyl diphosphate. *P Natl Acad Sci* **106**:10865-10870

Schillmiller AL, Schauvinhold I, Larson M, Xu R, Charbonneau AL, Schmidt A, Wilkerson C, Last RL, Pichersky E (2009) Monoterpenes in the glandular trichomes of tomato are synthesized from a neryl diphosphate precursor rather than geranyl diphosphate. *P Natl Acad Sci* **106**:10865-10870

Schwab, B., Folkers, U., Ilgenfritz, H. and Hülskamp, M. (2000) Trichome morphogenesis in *Arabidopsis*. *Philosophical Transactions of the Royal Society of London. Series B: Biological Sciences*, 355(1399), pp.879-883.

Shepherd RW, Bass WT, Houtz RL, Wagner GJ (2005) Phylloplanins of tobacco are defensive proteins deployed on aerial surfaces by short glandular trichomes. *Plant Cell* **17**:1851-1861

Szymanski DB (2005) Breaking the WAVE complex: the point of *Arabidopsis* trichomes. *Curr Opin Plant Biol* **8**:103-112

Szymanski DB, Jilk RA, Pollock SM, Marks MD (1998) Control of *GL2* expression in *Arabidopsis* leaves and trichomes. *Development* **125**:1161-1171

Szymanski, D. (2000) The Role of Actin During Arabidopsis Trichome Morphogenesis. *Actin: A Dynamic Framework for Multiple Plant Cell Functions*, pp.391-410.

Szymanski, D. (2005) Breaking the WAVE complex: the point of Arabidopsis trichomes. *Current Opinion in Plant Biology*, 8(1), pp.103-112.

Tian, D., Tooker, J., Peiffer, M., Chung, S. and Felton, G. (2012) Role of trichomes in defense against herbivores: comparison of herbivore response to woolly and hairless trichome mutants in tomato (*Solanum lycopersicum*). *Planta*, 236(4), pp.1053-1066.

Walker JD, Oppenheimer DG, Concienne J, Larkin JC (2000) *SIAMESE*, a gene controlling the endoreduplication cell cycle in *Arabidopsis thaliana* trichomes. *Development* 127:3931-3940

Watanabe, S., Mizoguchi, T., Aoki, K., Kubo, Y., Mori, H., Imanishi, S., Yamazaki, Y., Shibata, D. and Ezura, H. (2007) Ethylmethanesulfonate (EMS) mutagenesis of *Solanum lycopersicum* cv. Micro-Tom for large-scale mutant screens. *Plant Biotechnology*, 24(1), pp.33-38.

Williams WG, Kennedy GG, Yamamoto RT, Thacker JD, Bordner J (1980) 2-Tridecanone: A naturally occurring insecticide from the wild tomato *Lycopersicon hirsutum* f. *Glabratum*. *Science* 207:888-889

Yan A, Wu MJ, Zhao YQ, Zhang AD, Liu BH, Schiefelbein J, Gan YB (2014) Involvement of C2H2 zinc finger proteins in the regulation of epidermal cell fate determination in *Arabidopsis*. *J Integr Plant Biol* 56:1112-1117

Yang C, Li H, Zhang J, Luo Z, Gong P, Zhang C, Li J, Wang T, Zhang Y, Lu Ye,

Ye Z (2011) A regulatory gene induces trichome formation and embryo lethality in tomato. *P Natl Acad Sci* **108**:11836-11841

Zhao M, Morohashi K, Hatlestad G, Grotewold E, Lloyd A (2008) The TTG1-bHLH-MYB complex controls trichome cell fate and patterning through direct targeting of regulatory loci. *Development* **135**:1991-1999

Zhao Y, Pan Z, Zhang Y, Qu XL, Zhang YG, Yang YQ, Jiang XN, Huang SJ, Yuan M, Schumaker KS, Guo Y (2013) The Actin-related protein2/3 Complex regulates mitochondrial-associated calcium signaling during salt stress in *Arabidopsis*. *Plant Cell* **25**:4544-4559

Zhou WQ, Wang YC, Wu ZL, Luo L, Liu P, Yan LF, Hou SW (2016) Homologs of SCAR/WAVE complex components are required for epidermal cell morphogenesis in rice. *J Exp Bot* **67**:4311-4323

Zhou WQ, Wang YC, Wu ZL, Luo L, Liu P, Yan LF, Hou SW (2016) Homologs of SCAR/WAVE complex components are required for epidermal cell morphogenesis in rice. *J Exp Bot* **67**:4311-4323

Abstract in Korean

토마토에서 뒤틀린 모상체를 가진 돌연변이의 형태학 그리고 분자적 특성 규명

천재인

서울대학교 국제농업기술대학원 국제농업기술학과

지도교수 강진호

모상체는 식물체의 표면에 발달된 털 구조이며, 다양한 생물학적, 비생물학적 스트레스에 대한 물리적, 화학적 방어 기능을 하는 특징으로 잘 알려져 있다. 식물 방어에 있어 모상체의 역할이 매우 중요함에도 불구하고, 대부분의 다세포 모상체 형성에 관여하는 유전자는 밝혀진 것이 거의 없다. 따라서 토마토에서 모상체 발달에 관여하는 유전자를 동정하기 위하여 EMS 돌연변이 발생에 의해 생성된 Micro-Tom 돌연변이 집단을 선별하고, 야생종 토마토와 비교하여 뚜렷한 모상체 표현형을

가진 4 개의 돌연변이를 얻었다. 본 연구진이 선별한 모든 돌연변이는 이전에 알려진 *hl* 와 *ini* 돌연변이처럼 구부러지고 뒤틀린 모상체의 형태가 비슷하였다. 따라서, 본 연구진은 새로운 돌연변이를 *hl2*, *hl3*, *hl4*, *hl5* 로 명명하였다. 기존 연구에 따르면, *hl* 과 *ini* 는 액틴 세포골격의 중합화에 관여한다는 것을 밝혔고, 새로운 돌연변이가 이와 유사한 형태를 가진 것을 고려하여 새로운 돌연변이에 해당하는 유전자도 액틴 중합화와 관련이 있다고 가설을 세웠다. 가설을 증명하기 위하여, 액틴 중합화에 관여하는 ARP2/3 및 WAVE 복합 유전자에 대해서 16 개의 특정 프라이머 세트를 사용하여 네 개의 돌연변이 앞에서 RT-PCR 을 수행하였다. 모든 유전자는 wild-type 과 *hl5* 돌연변이 사이에 다른 조각 크기를 보인 *ARPC1* 유전자를 제외하고 모든 돌연변이에서 예상 크기로 증폭되었다. *ARPC1* 유전자의 cDNA 와 gDNA 염기서열 분석 결과, *hl5* 돌연변이의 9 번 intron 의 5'-donor site 에서 G 를 A 로 치환되어 망가진 것을 확인하였다. *hl5* 돌연변이에 야생종 *ARPC1* 유전자를 발현시킨 결과, 정상적인 모상체가 발달되었다. 이러한 결과는 *hl5* 돌연변이가 액틴 세포골격 형성에 문제가 있었다는 것을 증명한다.

주요어 : 액틴, ARP2/3 및 WAVE 복합체, ARPC1, *Hairless*, 토마토, 모상체

학 번 : 2017-23619

